DOSIMETRIC COMPARISON BETWEEN TWO TREATMENT PLANNING SYSTEMS FOR DCAT IN SINGLE AND MULTI-LESION PATIENTS

By

John T. Berzanske IV

A THESIS

Presented to the Department of Medical Physics
and the Oregon Health & Science University
School of Medicine
in partial fulfillment of
the requirements for the degree of
Master's of Science

May 2021

TABLE OF CONTENTS

List of Figures

List of Tables

Abbreviations

CBCT: Cone beam computed tomography

CI: Conformity index

DCAT: Dynamic conformal arc therapy

GI: Gradient index

IPCI: Inverse Paddick conformity Index

IQR: Interquartile range

MU: Monitor units

OAR: Organ at risk

PCI: Paddick conformity Index

PIV: Planned isodose volume

PTV: Planning treatment volume

QA: Quality assurance

SBRT: Stereotactic body radiation therapy

SRS: Stereotactic radiosurgery

TPS: Treatment planning system

TTV: Treated target volume

Acknowledgements:

I would like to thank my advisors Dr. Boopathy and Dr. Heard for their input and guidance through the process of the project. I would also like to thank Dr. Griglock and Dr. DeWeese for their advice and the excellent graduate student advocacy system. I extend my gratitude to Dr. Pugachev for also serving on my committee and contributing thoughtful feedback. Lastly, I thank my family for their consistent support and classmates for their fellowship along the way.

Abstract:

Purpose: This work is concerned with the comparison of two different dynamic conformal arc therapy (DCAT) stereotactic radiosurgery (SRS) planning systems, namely Eclipse and BrainLab Elements. The creation of an SRS plan is an involved process with many parameters to be considered and the treatment efficacy is sensitive to the accuracy of its delivery. As a result, the process of effective plan creation with acceptable normal tissue and organ at risk (OAR) sparing can be time consuming. The Elements treatment planning system (TPS) offers a streamlined approach to creating cranial SRS plans. The intention of this study is to dosimetrically compare each system to understand any potential gains in utilizing the Elements TPS.

Methods: The study used 10 patients with 15 different single lesions to be treated with cranial SRS. Clinical treatment plans were initially created in Eclipse and received patient specific quality assurance (QA) before being delivered to patients. A second set of plans with the same prescription dose, matched arc lengths, couch positions, and coverage were created in the BrainLab Elements planning system. These plans then received patient QA. Comparative analysis of both sets of plans and their respective QA was based on inverse Paddick conformity index (IPCI), gradient index (GI), dose to organs at risk (OAR), gamma analysis of the QA, total monitor units (MU) delivered, and the volume of brain receiving at least 12 Gy (V_{12}). Significance of statistical difference was evaluated using the non-parametric Wilcoxon signed-rank test given the non-normal distribution of the data due to the population of less than 20 at n=15.

Results: Inverse Paddick conformity indices of the Elements plans averaged within the ideal range of less than 1.18 while the Eclipse plans delivered just outside of the range at 1.19 with no significant statistical difference. Gradient indices of the Elements plans were found to have significant statistical difference from the Eclipse plans with an average 6.41% decrease in value. The parameter V_{12Gy} was reduced by 2.67% to 27.14% in 13 of the 15 Elements plans. D_{max} delivered to OARs was on average 12.19% higher in the Elements plans, affecting the brainstem immediately adjacent to the lesion in one case. For individual structures including the eyes, optic nerves, and chiasm, most increases were well within OAR tolerance. Gamma analysis of the Elements patient QA plans showed equal or better coincidence to every Eclipse plan. There were no significant differences in the total planned MUs.

Conclusion: The Elements TPS offers an efficient process for rapidly creating serviceable SRS plans and was able to create treatment plans dosimetrically comparable to Eclipse plans in as few as 15 minutes, with an established structure set. Conformality was found to be effectively the same between the systems with Elements leading in performance with respect to the GI and V_{12Gy} parameters. Investigation of the Elements trajectory optimization process is beyond the scope of this work. Further study should be completed, expanding the use of the software optimizations and the potential impact on increases in D_{max} across OARs.

1. Introduction

Stereotactic radiosurgery (SRS) and stereotactic body radiation therapy (SBRT) are precise radiation treatment approaches used to address cancerous lesions and abnormalities of the body. These conditions are often located in anatomically challenging places that would be difficult to reach with other methods of treatment like surgery. The advantage of SRS is the high level of precision in treatment delivery paired with the noninvasive nature of external beam radiation therapy. External beam radiation therapy lacks the medically intrusive characteristics of traditional surgical procedures. This makes SRS of particular use when treating head and neck cases where more invasive procedures are difficult to execute and can carry higher risks [1].

An SRS treatment is the delivery of typically 15-22 Gy in a single fraction or treatment [2]. This differs from other conventional radiation fractionation schemes that can spread the radiation dose out over many weeks. Fractionation in this manner essentially allows for a large dose of radiation to be delivered while maintaining an acceptable maximum level of normal tissue toxicity in the process. Staying below this level acceptable toxicity allows for normal tissue to repair and recover while the tumor volume sustains accruing tissue damage [3]. This also differs from other central nervous system treatments like whole brain radiation therapy (WBRT). These treatments irradiate the entire brain and have impacts on neurocognitive function. The large, single fraction dose gives effective brain disease control, especially when coupled with SRS or surgery, but can lead to problematic late side effects [4].

Historically, in order to maintain the precision of the treatment, SRS patients would need to be immobilized and positioned using a large head frame. This method still exists but in many institutions this process has been replaced with the image guided radiation therapy procedures to position the patient in conjunction with a thermoplastic immobilization mask. Here, the

positioning is completed by imaging the patient and using those images to create a treatment plan. Immediately before delivering that plan, the patient is then reimaged, often with cone beam computed tomography (CBCT). Software then takes the new image data and the original treatment planning image data to and processes them to localize where the tumor and treatment volumes are in three-dimensional space, as well as the relevant other structures and organs at risk (OAR). At this point, the treatment delivery system can deliver the prescribed dose to volume within millimeter precision.

Conditions found to be eligible for SRS treatment are planned for by utilizing software to organize, calculate and execute each part of the treatment plan. This is done to take advantage of computational power to process the sophisticated dose delivery calculations. Here, the complexities of attenuation, scatter, beam and gantry angles, patient topology, and many other contributing factors can be efficiently assessed all through a contained process. Of the many existing treatment planning systems, each has their own approach to this process with different beam models and algorithms and different features useful for yielding deliverable plans. The accuracy of dose delivery is of particular concern when addressing SRS plans.

There are different methods of delivering the radiation treatment to the patient. One expedient approach is to use dynamic conformal arc therapy (DCAT). This modality is useful in that the plans are quickly assembled and delivered. The method involves the conforming of the multileaf collimator (MLC) leaves fitting to the treatment site from the perspective of the beam as the treatment moves in an arc across the patient. For treatment sites that have simple spherical or ellipse geometries, the MLC is easily capable of meeting the mechanical requirements of the plan. The result is a lower level of required QA due to the linear accelerator operating well within its mechanical capabilities. However, not all treatment sites have simple geometries, and

some are inconveniently proximal to sensitive tissues and organs. Here, volumetrically modulated arc therapy (VMAT) can be useful. VMAT plans rely on the summation of modulated beams to accomplish target coverages. This can advantageous when working in constricted and compact anatomy like the head and neck. However, because VMAT results in increasingly more complicated fields shapes, a higher level of QA must be completed to confirm that the designed treatment with the irregular field shapes will be able to be successfully delivered on the treatment machine. Additionally, the plans themselves can take longer to calculate and the reliance of the planning on the dose calculation models in conjunction with the potential use of very small, modulated field sizes may overestimate the accuracy of the calculation itself. Many assumptions are made in dose modelling and those assumptions may become more inaccurate as the field size scales down.

When creating an SRS DCAT plan, consideration for the geometry of the beam delivery is important. The process of treatment design is effectively choosing the best paths through which beams of radiation can pass through, rotating about the intersection point at the isocenter for some angle for each beam, concentrating the dose to a point at the PTV. Such a large, potentially single fraction dose delivered to the treatment site via these beams means that any tissues in any of the beam paths may be heavily irradiated. This includes normal tissue and potentially radiosensitive organs. Consequently, different combinations of couch angles and ranges of gantry movement are arranged to best maximize avoidance of these normal structures. The process of doing so is a combination of experience and training coupled with testing assembled plans in the software environment to check the expected dose distribution. In short, some level of trial and error is involved as every patient case is different. Templates containing

typical combinations of couch angles and arc lengths can be stored to add efficiency to the planning process, but these are only starting points for the treatment planning.

The DCAT component of the treatment describes the conformality of the collimator leaves around the treatment site. As the beam moves through each arc, the collimator leaves are shaped to fit to the treatment volume from the perspective of the beam's eye view, effectively blocking beam radiation to normal tissue and other structures while allowing the PTV to be irradiated. The collimator leaves will fit to the PTV shape better in some orientations and worse in others, so initial collimator angle must also be considered when choosing a beam arc. Also, because the beam has an exit path after passing through the PTV, dosage can be delivered to normal tissue on the other side of the treatment site and so even further consideration should be given when choosing the beam trajectories with couch angles and arc lengths.

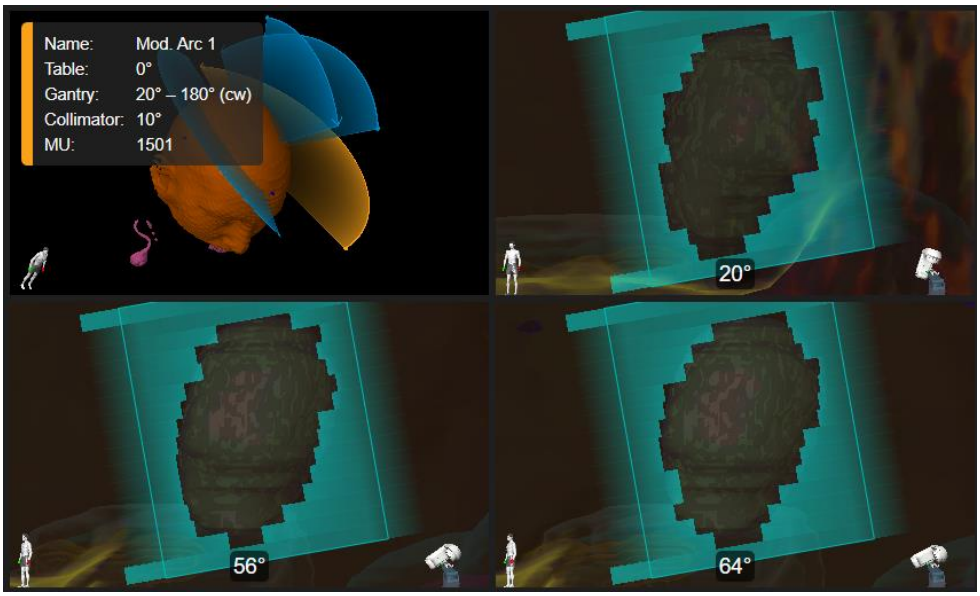

Figure 1: Image of the MLC conforming to the target volume as moves through its path. The leaves are adjusting to fit to the edges, though a perfect fit is not possible due to the limiting rectangular geometry of the leaves contrasting with the rounded edges of the treatment volume. As such, choosing appropriate collimator rotation angles is necessary to achieve the most conformal results.

The purpose of this thesis is to dosimetrically compare the treatment planning system of Eclipse with the BrainLab Elements planning system, specifically looking at the Cranial SRS module. The Eclipse system is robust and clinically proven, with a great deal of control over the planning process. Its workflow intricacies, however, require a steep learning curve and require thorough experience and training to be able to effectively and efficiently implement. The Elements system, also clinically proven, takes a different approach by breaking up the process of SRS planning into smaller pieces with a distinct workflow. It uses predetermined protocols with defined prescriptions and beam arrangements as a starting point for plan design and employs auto-contouring to shorten the treatment setup time. The streamlined approach is an attempt to create consistent and deliverable SRS plans, regardless of the user's experience, while increasing the number of patients that can be treated. This study aims to evaluate those criteria prior to implementation at OHSU.

When planning SRS DCAT treatments in the Eclipse system, it is typical to start with a template of arcs, including typical gantry rotation ranges over a number of couch positions as well as a prescription dose over a number of fractions, and as few as one. These templates are then checked in the current patient anatomy to see where exactly the paths of the beams will be. A simple approach to this is stepping through the beam motion while viewing from the beam's eye view. This allows the planner to see where the pointing as it moves through and rotates about the PTV.

Toggling other objects in the contoured structure set on and off makes it possible to view the position of those other structures with respect to beam's movement and allows the planner to appropriately choose starting and stopping angles, as well as situations where the single arc may need broken into two arcs in order to avoid OARs. For instance, when treating lesions near the

optic chiasm it can be beneficial to break an arc into two in order to avoid the chiasm. Blocking can also be employed where the collimator leaves will move into place from the conformation about the PTV edge to block tissue.

Each of these arcs delivers dose through a plane crossing through the isocenter. The combination of all the arcs concentrates the dose at the isocenter but obviously, dose will also exist within and about the planes as well. The accumulation of all the doses will result in a three-dimensional volume of dose distribution. The shape of this distribution can be influenced by changing the weights of the different fields. Reducing the weight of a particular arc can help control unwanted streaks of dose through tissue. A disadvantage to the practice, however, is that the leaves may not perfectly match the structure needing blacked and a finite some amount of time is required to move the leaves into places. For a gantry with a fixed rotation speed, this means that the leaves will be moving from the conformal configuration into a blocking configuration for some part of the path, potentially altering the target coverage.

Planning SRS treatments in the Elements system has some similarities to the Eclipse process. Eclipse utilizes protocols with different sets of arcs in different couch positions. For instance, a protocol might be “3 arcs left” where there are three arcs, and the couch positions adjust them such that the arcs cover the left side of head. The protocols also include a prescription dose and fractionation scheme, like 2000 cGy in a single fraction, that can be edited for a particular case once implemented.

Each TPS uses a different dose calculation model. The Eclipse plans were calculated using the Acuros XB algorithm while the Elements plans were completed using a pencil beam algorithm [5,6]. The pencil beam algorithm is a fast correction-based algorithm and operates on the assumption that the cumulative delivery beam is composed of smaller pencil-like beams

adjacent to each other. Each of the smaller beams contributes a dose in the medium it's incident upon. The Acuros XB is a linear Boltzmann transport equation solver algorithm that addresses the heterogeneities in dose calculations. The accuracy of the resulting calculations is comparable to the results of a Monte Carlo simulation but yielding results in a much shorter time.

Before the start of the study, each Eclipse treatment plan was created using a manual approach. The dosimetrist creating the plan used contours created by the patient's physician based on the CT and MR image data captured for the planning process. The structure contours included the relevant anatomical structures, OARs, PTVs and GTVs. A prescribed dose and fractionation scheme was chosen by the physician.

With these parameters in consideration, the dosimetrist manually selected the couch positions and the arc angles of rotation for each position. A template of arcs and couch positions could be selected to increase efficiency in the initial plan setup, allowing for adjustments of the generic treatment geometries instead of creating from scratch. However, as each patient treatment scenario varies, it was still sometimes necessary for the dosimetrist to add or remove fields, or potentially break a single arc into two arcs in order to avoid structures. Arc length minimum was set to 30 degrees.

As the arcs were created, the fit and shield function was often used to create margins of 1 or 2 mm around structures that needed to be blocked from the treatment beam. For consistency of practice and form, a margin of 5 mm was typically chosen between lesions when creating an arc. MLC angle steps were typically set to no larger than 2 degrees, though one patient had the steps set to 2.8 degrees. A conformity index goal of less than or equal to 1.2 was considered acceptable outside of cases where the treatment volume was particularly jagged or irregularly shaped. In those cases, a conformity index goal of 1.5 or less was considered acceptable. The

gradient measure is the difference between the radii of the equivalent spheres of the 50% and 100% isodose line volumes measured in cm. A typical level of less than 0.4 was considered acceptable.

Each arc was followed through the beam's eye view to clarify what objects aside from the treatment volume might pass through the beam. Adjustments in arc length, couch position and blocking were made at this point, where necessary. In patients with more than one treatment volume, the other volume was also avoided when choosing a beam arc.

In general, adjusting the weights of the fields could be used to adjust the three-dimensional geometric distributions of the dose. Increased field weight along an arc would result in increased dose about the plane that arc moves through. Likewise, dose coverage could be adjusted and normalized to further impact the conformity index and gradient index. Normalizing to a higher percentage of coverage could be used to increase the conformity index.

The Eclipse planning process was highly tailored to each patient and required the manual control of most parameters in the planning process. Although some functions like fit and shield as well as generic treatment templates of couch positions and field angles could be used to increase efficiency, decision making concerning the arc length, breaks in the arcs, couch position adjustments, and collimator positions still had to be carried manually while critically thinking about the plan. This increased in complexity for patients with more than one lesion each being treated separately.

2. Material and Methods

2.1 Instrumentation and equipment

Prior to the start of the study, a series of ten patients were treated with dynamic conformal arc therapy (DCAT) for a total 15 single brain lesions. The clinically delivered treatments were planned on the Eclipse treatment planning system version 15.1 using the Acuros XB dose algorithm with 0.1 cm grid resolution. Beam energies for the clinical plans were chosen to be 6 MV flattening filter free (6X FFF). The plans were created manually choosing the gantry and collimator angles as well couch positions and the number of arcs specifically for each patient's specific condition. The number of arcs ranged from three to five and all prescription doses were delivered in a single fraction except for patient number two who received the dose in three fractions.

New duplicate plans were created in the BrainLab Elements system using the cranial SRS module version 1.5. The process began with exporting the exact structure sets from the Eclipse TPS to the Elements TPS. Keeping the structure sets identical removed them as a variable and allowed for the comparison of other TPS performance criteria without the influence of variation in contours between the systems.

Elements has several optimization algorithms including trajectory optimization, normal tissue sparing optimization, modulation scaling, and weighting optimization. Each of these optimizers have an adjustable parameter slider that weights the feature optimization towards one of two optimization situations with the slider values in between reflecting some blend of the two.

The normal tissue sparing optimization toggles the presence of an unseen ring object in the structure set. The ring object has 35 mm thickness that surrounds but does not include the PTV. The optimizer uses the ring object to impact the gradient of the dose delivery. As the

normal tissue sparing setting values are moved from low to high, the algorithm demonstrates increased control over the tissue within the ring resulting in improved gradient and conformity indexes. Because Elements allows for structures designated as OARs to have their own dose constraint parameters, altering the normal tissue sparing values is a way to impact the sparing of tissues more directly near and the OARs without altering the sparing of the OARs themselves.

The weighting optimization can be varied to impact the importance of either the target coverage or the OAR sparing over the other. Varying the slider will adjust the balance and cause the optimization algorithm to change the weighting priority so as the target coverage is increased, the OAR sparing is potentially compromised and decreased. Similarly, as the OAR sparing is increased, target coverage is prioritized less and can potentially decrease. The slide allows for quick recalculations to efficiently compare the balance of the two criteria. The option sets the importance of reducing modulation and given that these plans are DCAT, dose modulation is not desired. Setting the value to low eliminates modulation between control points and while it is not a true DCAT plant, this setting approximated a DCAT with manually adjusted leaf positions. All the Elements plans were completed with the modulation setting selected to the low position given the desire to compare a DCAT Eclipse plan to a DCAT Elements plan. Because of this, no trajectory optimization was implemented and the number of arcs, arc lengths, collimator starting positions, and couch positions were exactly matched to values used in the Eclipse plans.

Figure 2. The Elements TPS utilizes optimizations that include the balance of target weighting to OAR weighting, normal tissue sparing which uses a hidden ring object and modulation which varies the plan from a conformal approach to a modulated approach.

2.2 Elements plans with matched geometry

The structure sets and image data from each of the Eclipse plans were exported to BrainLab Elements. These sets included the contoured anatomical structures including the brainstem, both cochleae, both optic nerves, the optic chiasm, the eyes, the lenses, as well as the PTV and GTV. The GTV is the tumor volume that came be imaged and seen. Its volume, shape, and position are expected to specify the tumor. This differs from the PTV which is a volume selected to enclose the GTV and account for inaccuracies in beam positioning and delivery as well as potential internal anatomical misalignment. Other control structures present in the Eclipse environment, like rings for example, were not utilized in the Elements planning environment as the normal tissue sparing algorithm would be used instead. In the Eclipse

planning system, these structures are in place to assist in controlling the dose distribution within the patient volume and impact normal tissue sparing. Their omission in the Elements environment was done so that the optimization capabilities of the Elements software would be able to operate acting upon the PTV alone.

Once the structure sets and image data were accessible in the Elements planning environment, the plan creation process was as follows. First, the patient was selected via name and ID number. From there, the cranial SRS module was selected from the SRS section of the planning choices. A timeline of data was presented including the image data and the structure sets. These are sorted by date created along an actual timeline for ease of navigation. Here, combinations of data can be selected together. For instance, a CT image set and the related structure set. It's also possible to omit objects within a set. For each patient, the relevant image data and structure set including the OARs, PTV and GTV were selected.

From this point, the Elements plan creation process is broken up into viewing, co-registration, contouring, dose planning and review sections.

The viewing section contains only one element which is the viewer. Entering it allows the user to quickly check that the corrected structures were opened and are correctly oriented within the image data. It's possible to scroll and add views more than the default axial view. Measurements can be taken using the measuring tools in the sidebar and comparisons can be done by opening other patient data. This section was used as a quick verification of structure set selection for all treatment plans created.

The next section, co-registration, contains two elements. The first is to handle image fusion and the second is to handle image distortions. Neither of these elements were necessary or used in the treatment plan creation process.

Next was the contouring section. Here there were three elements. The first was actual contouring and the element was entitled anatomical mapping. Here, auto contouring could be used to detect and contour common head and neck structures. Because the goal was to compare the Eclipse treatment plans directly to Elements treatment plans for the same patients, the exact Eclipse structure set that imported to Elements was used instead of this auto contouring function. The related smart brush element for additional contouring was also omitted in this study.

The object manipulation element was used to assign the object type and object role to each structure. For instance, the imported eye lenses were assigned the type of left and right lens for each, and their roles were assigned as OAR so that they could be considered in the optimization process. Similarly, each imported PTV and GTV structure was assigned the correct role of PTV and GTV. Further contouring could be completed in this section but was not so as to preserve the matching structure set geometry between planning systems.

Table 1. Structures imported from Eclipse to Elements and their assigned object type and role.

Imported structure	*Object type*	*Object role*
Brain	Brain	-
Brainstem	Brainstem	OAR
Left eye	Left eye	OAR
Right eye	Right eye	OAR
Left optic nerve	Left optic nerve	OAR
Right optic nerve	Right optic nerve	OAR
Left lens	Left lens	OAR
Right lens	Right lens	OAR
Spinal cord	Spinal cord	OAR
Optic chiasm	Optic chiasm	OAR
PTV	PTV	PTV
GTV	GTV	GTV

The cranial SRS element in the dose planning section was then used to create the treatment plans. For each treatment, the couch model was selected to none. The HU to electron density table was selected to be the CT_CCC_Philips option. The treatment orientation was supine, head to gantry. Once the tissue model was created in the next section, parameters of the treatment could be selected. A machine profile for the Varian TrueBeam was selected as well as a beam profile of 6.0 MV FFF. For each patient, a treatment protocol with the same number of arcs as its Eclipse plan was selected.

By enabling advanced editing, these protocol arc lengths, couch positions, and starting collimator positions were able to be edited to exactly match the Eclipse plans. Advanced editing also made it possible to match the prescription dose by editing the PTV parameters. Here, the coverage percentages were also edited by changing the desired and tolerated volume covered percentages to the percentage covered specified in the Eclipse plan. The SRS prescription (controlled inhomogeneity) option was selected for the PTV. The primary OAR was selected to be the brainstem in all plans initially.

Table 2. Specific arc count, gantry rotation angle and couch position in degrees for each plan where CW denotes a clockwise gantry rotation and CCW denotes a counterclockwise rotation. Plans ranged from 3-5 arcs and couch positions.

	Arc 1		Arc 2		Arc 3		Arc 4		Arc 5	
	Gantry (°)	Couch (°)	Gantry (°)	Couch (°)	Gantry (°)	Couch (°)	Gantry (°)	Couch (°)	Gantry (°)	Couch (°)
1	200 CW 340	0	109 CW 179	0	310 CCW 200	45	40 CW 160	270		
2	200 CW 160	0	160 CCW 30	270	20 CW 130	315	330 CCW 220	45		
3	181 CW 179	0	145 CCW 25	300	335 CCW 215	60	-	-		
4	181 CW 179	0	185 CCW 25	315	335 CCW 215	65	-	-		
5	330 CCW 234	0	180.1 CW 310	53	25 CW 155	270	135 CCW 15	310		
6	0 CCW 246	0	200 CW 340	55	20 CW 160	270	135 CCW 15	40		
7	345 CCW 185	355	180.1 CW 300	60	25 CW 145	280	179.9 CCW 20	325		
8	160 CCW 20	0	20 CW 160	320	120 CCW 20	270	0 CCW 240	40		
9	330 CCW 210	0	200 CW 340	45	0 CW 90	270	155 CCW 25	325		
10	160 CCW 70	0	270 CCW 190	0	185 CW 305	55	25 CW 155	270	170 CCW 90	325
11	179.9 CCW 20	0	62 CW 179.9	302	125 CCW 55	270	340 CCW 190	30		
12	302 CCW 244	0	210 CW 340	45	20 CW 150	270	155 CCW 25	310		
13	179 CCW 29	0	250 CCW 190	0	200 CCW 340	45	20 CW 160	280	160 CCW 20	325
14	340 CCW 200	0	200 CW 340	37	0 CW 140	270	179.9 CCW 20	315		
15	160 CCW 210	0	200 CW 340	40	0 CW 170	270	150 CCW 40	315		

The primary OAR has its own parameters of a $D_{10\%}$ and a D_{max}. The default values are based on what the object type has been assigned as. Selecting advanced editing made it possible to alter these values, though they were initially left to their defaults. The $D_{10\%}$ and D_{max} fields had their own sliders with settings of off, smart. The off position would not consider the values, the smart position would have the algorithm employ consideration of the constraint, and the strict setting would cause the algorithm to consider the constraint a hard limit. All other OAR objects have guardian and D_{max} sliders that function similarly but with secondary priority to the primary OAR.

In each of the plans, the modulation slider was in the leftmost position set to low in order to prevent modulation between control points and approximate a true DCAT plan. The weighting and normal tissue sparing sliders were initially left at the center position. Each plan was then

calculated. Whether each constraint and parameter were met was indicated with a colored circle beside the structure and that parameter. A green circle indicated that the constraint was within tolerance. A yellow circle meant that the constraint was approaching the tolerance and a red circle meant that the constraint was not met. In instances where the constraints were not met, the weighting and normal tissue sparing parameters were adjusted to meet the constraint, as well as the smart and strict setting on the primary OAR. There were no instances where the secondary OARs required constraint adjustments.

Inverse Paddick conformity index data was collected from the Elements treatment planning system directly.

$$CI = \frac{PTV \cdot PIV}{TTV^2}$$

Here the PTV is the planning treatment volume, the PIV is the prescribed isodose volume and the TTV is the treated target volume [7]. Both systems have the capability to calculate the indices within the software with respect to the PTV but because Elements calculates the specific IPCI, measurements were later taken in the Eclipse software to calculate its own IPCI. Similarly, the GI can be collected directly from the Elements software whereas the 50% and 100% isodose volumes had to be measured from the DVHs in Eclipse to calculate the GI.

The inverse Paddick conformity index was used because it addresses the shortcoming of the computing conformity as a ratio of the treated volume to the PTV, when the PTV is completely within the treatment volume. The issue is that while the ratio will provide information about volumetric conformity, it does not address the orientation or shape of the volumes with respect to each other. The Paddick conformity index corrects for this including multiplying the ratio by the selectivity index. The selectivity index is simply the ratio of volume of the PTV covered by the 100% isodose line to the total volume enclosed by the 100% isodose

line. An ideal selectivity index would be greater than 0.9. An ideal PCI would be greater than 0.85 [10].

The GI is important as it gives indication as to how fast the dose falls off moving away from the treatment volume through normal tissue and nearby OARs [8]. As the 50% isodose volume gets smaller and approaches the 100% isodose volume, the ratio of 50% PIV to 100% PIV approaches the value of one. For larger values of the 50% isodose volume, the ratio is also large and indicates slower dose fall off. The volumes of V_{12Gy} were measured in each TPS using the dose volume histograms and the values of D_{max} were collected from the software given measurements.

2.3 Patient QA for each set of plans

The clinical patient QA of each plan was delivered on a Varian TrueBeam linear accelerator, serial #4180. A Sun Nuclear StereoPHAN phantom was used with a Sun Nuclear SRS MapCHECK high density diode array, model 1179 and serial #243843006, to measure the beam dose distribution. The StereoPHAN is an end to end phantom capable of housing a variety of detectors, including the MapCHECK which is a modern alternative to the much more time-consuming film patient QA approach. Its dense diode array is useful for fields at the 77mm x 77mm scale and suitable for SRS scenarios.

The SteroPHAN phantom was physically aligned to the isocenter using the room lasers. The treatment delivery data was then collected using Sun Nuclear SNC Patient software. Dose and plan RT files for patient QA exported from the Eclipse and Elements systems were imported into the SNC software. The RT files contain the actual treatment delivery data and once imported were able to be used to deliver the calculated treatments to the phantom. Treatment data was then

collected while the beam was on using the phantom and MapCHECK combination. The MapCHECK was connected to the Sun Nuclear Patient software operating in the SRS MapCHECK module. Here, the measured dose was collected and once all the fields of a plan were delivered, the measured plan was then able to be compared to the imported calculated plan within the software. Gamma analysis was used to compare the calculated data set to the measured data set. The analysis is a built-in function of the software with parameters that can be edited to suit the needs of the treatment being measured. Each point of measurement in the collected plan can be compared to the same point in the calculated plan to look for a percentage variation. Similarly, the dose at each point can be analyzed to measure the distance from that point to another point with the same dose measurement value. This distance is called the distance to agreement. Gamma analysis was recorded for every combination of 2% and 1% difference at a point and 1mm, 2mm, and 3mm distance to agreement. OHSU and many other institutions typically use the criteria 3% dose difference and 1 mm distance to agreement when evaluating SRS cases.

3. Results

Table 3: Each of the PTV values and their respective prescription doses given in cGy. It can be seen that for increasing size of tumor volume the prescription dose decreases to as low as 1500 cGy for the 9.79 cm^3 tumor.

	PTV (cm^3)	Prescription dose (cGy)
1	2.09	2000
2	0.45	2000
3	0.29	2000
4	0.66	2000
5	0.37	2000
6	1.28	2000
7	0.27	2200
8	0.39	2200
9	0.2	2200
10	0.13	2200
11	9.79	1500
12	3.92	1800
13	4.53	1600
14	0.59	2000
15	1.88	2000

PTV values ranged from very small at 0.2 cm^3 to 9.79 cm^3. More than half of the dose prescriptions were a standard 2000 cGy while the other seven ranged from 1500 to 2200 cGy. In one instance the fractionation scheme was patient was originally three separate fractions. In order to compare the new Elements plan to the fractionated Eclipse plan, a new Eclipse plan was created with the exact same parameters except the prescription dose was normalized to a single fraction. This enabled the plans to be compared directly.

Table 4: Summary of comparison parameter statistics between the Eclipse and Elements treatment planning system results for n=15 cases where IQR is the interquartile range and W is the Wilcoxon test statistic. Values of W denoting statistically significant differences between the treatment plans are represented in bold. RT is right, LT is left, opt is optic.

	Eclipse				Elements				
	Mean	Std Dev.	Median	(IQR)	Mean	Std Dev.	Median	(IQR)	W
Inverse Paddick Conformity Index	1.19	0.11	1.19	0.04	1.16	0.11	1.12	0.06	34
Gradient Index	3.43	0.74	3.45	0.32	3.21	0.45	3.42	0.17	**25**
V_{12Gy} (cm^3)	3.52	3.82	1.69	3.13	3.31	3.53	1.57	3.24	**8**
MU	3718.27	563.27	3794.00	369.00	3630.27	399.64	3570.00	305.00	40
Brainstem Dmax (cGy)	278.32	577.76	49.00	44.70	304.47	589.91	71.00	49.00	**4**
Right cochlea D_{max} (cGy)	135.23	333.74	8.40	20.40	150.60	384.50	13.00	19.00	**14**
Left cochlea D_{max} (cGy)	21.27	41.13	3.30	9.60	25.80	44.63	7.00	10.50	**9.5**
Right eye D_{max} (cGy)	4.89	4.11	3.60	3.10	8.07	5.35	8.00	4.00	**0**
Left eye D_{max} (cGy)	4.96	5.84	3.60	0.75	8.67	8.98	4.00	7.00	**6**
Right opt. nerve D_{max}(cGy)	33.15	41.97	12.70	32.00	36.40	37.25	16.00	49.00	28
Left opt. nerve D_{max} (cGy)	25.15	23.63	16.20	17.10	28.53	22.43	21.00	15.50	**24**
Chiasm D_{max} (cGy)	78.86	125.45	29.70	51.10	89.40	122.76	47.00	58.50	**9**

The summary statistics were calculated by first checking for normal distribution of the datasets. This was accomplished by using a Shapiro-Wilk test with a significance level of $\alpha = 0.05$. The test is computed using a null hypothesis stating that the sample is pulled from a population with normal distribution [9]. Each population of data was written to an array in the Python integrated development environment and the Shapiro-Wilk test was run using the Shapiro()SciPy function of the SciPy package. In general, data was not normally distributed, likely due to the number of cases being less than 20. As the comparison between the treatment planning systems was concerned with the same plans having the same delivery geometries on two different planning systems, the resulting data for each comparison parameter required a non-parametric paired test to determine significant statistical variance. The Wilcoxon signed-rank test was used to test for statistical difference with a Wilcoxon critical value of 25 for the population

of n=15. The z and p values were also calculated but disregarded as the population was less than 20.

The inverse Paddick conformity index is given by IPCI =[(GTV)(PIV)]/TTV^2 where TTV is the treated target volume and PIV is the prescription isodose volume or the volume within the 100% isodose line. This is the inverse of the product of the undertreatment and overtreatment ratios. The conformity index collected in Eclipse is as defined in ICRU as CI = TV/PTV where TV is the treated volume and PTV is the planning treatment volume. In order to compare the conformity of the treatments directly, the PIV and TTV were measured in the Eclipse software to compute the iPCI.

The gradient index given by the ratio of the volume enclosed by the 50% isodose line and the 100% isodose line. The value is obtained directly within the Elements software. In the Eclipse software, the 50% and 100% isodose volumes were measured and used to calculate the GI for each plan.

The total MUs delivered were obtained directly from each software.

Table 5: D_{max} in cGy delivered to the right and left cochlea, and the right and left eyes in each planning system. The % represents the percentage change from the Eclipse system to the Elements system.

	Right cochlea			Left cochlea			Right eye			Left eye		
	Eclipse	Elements	Difference	Eclipse	Elements	Difference	Eclipse	Elements	Difference	Eclipse	Elements	Difference
1	1143.3	1413.0	269.7	98.3	118.0	19.7	6.7	12.0	5.3	4.4	11.0	6.6
2	2.4	5.0	2.6	2.6	5.0	2.4	1.3	3.0	1.7	3.1	4.0	0.9
3	0.7	3.0	2.3	0.5	3.0	2.5	0.6	2.0	1.4	0.6	2.0	1.4
4	27.3	32.0	4.7	27.3	26.0	-1.3	0.9	4.0	3.1	0.9	4.0	3.1
5	21.0	29.0	8.0	1.5	4.0	2.5	2.4	3.0	0.6	0.8	3.0	2.2
6	30.3	32.0	1.7	1.9	7.0	5.1	5.6	8.0	2.4	3.7	6.0	2.3
7	2.3	3.0	0.7	0.8	3.0	2.2	2.7	3.0	0.3	1.0	3.0	2.0
8	5.1	8.0	2.9	2.5	5.0	2.5	2.0	4.0	2.0	2.4	4.0	1.6
9	35.1	36.0	0.9	3.3	5.0	1.7	14.5	16.0	1.5	3.6	3.0	-0.6
10	16.8	19.0	2.2	13.9	11.0	-2.9	6.7	8.0	1.3	21.1	37.0	15.9
11	8.4	13.0	4.6	141.3	149.0	7.7	10.2	12.0	1.8	16.4	16.0	-0.4
12	723.0	639.0	-84.0	11.9	20.0	8.1	9.9	16.0	6.1	4.3	11.0	6.7
13	4.2	11.0	6.8	5.5	12.0	6.5	3.6	11.0	7.4	4.7	11.0	6.3
14	3.8	6.0	2.2	1.1	4.0	2.9	1.0	3.0	2.0	3.2	3.0	-0.2
15	4.7	10.0	5.3	6.6	15.0	8.4	5.2	16.0	10.8	4.2	12.0	7.8
	Ave change:		11.37%	Ave change:		21.32%	Ave change:		65.08%	Ave change:		74.73%

Table 6: D_{max} in cGy delivered to the left and right optic nerves, the optic chiasm and the brainstem in each planning system. The % represents the percentage change from the Eclipse system to the Elements system.

	Left optic nerve			Right optic nerve			Chiasm			Brainstem		
	Eclipse	Elements	Difference	Eclipse	Elements	Difference	Eclipse	Elements	Difference	Eclipse	Elements	Difference
1	12.7	16.0	3.3	91.2	91.0	-0.2	148.1	147.0	-1.1	2121.1	2134.0	12.9
2	6.8	9.0	2.2	13.2	9.0	-4.2	53.7	51.0	-2.7	88.2	82.0	-6.2
3	1.9	5.0	3.1	2.5	6.0	3.5	20.8	41.0	20.2	23.6	43.0	19.4
4	3.2	5.0	1.8	2.4	5.0	2.6	4.4	6.0	1.6	43.0	48.0	5.0
5	32.9	55.0	22.1	20.0	34.0	14.0	22.7	36.0	13.3	65.9	112.0	46.1
6	10.0	16.0	6.0	25.1	33.0	7.9	29.7	41.0	11.3	47.9	62.0	14.1
7	6.1	12.0	5.9	16.2	21.0	4.8	29.4	52.0	22.6	47.9	86.0	38.1
8	17.8	29.0	11.2	7.5	7.0	-0.5	21.7	34.0	12.3	48.5	71.0	22.5
9	20.7	19.0	-1.7	41.5	46.0	4.5	45.2	47.0	1.8	37.0	43.0	6.0
10	114.2	102.0	-12.2	13.6	19.0	5.4	78.7	96.0	17.3	43.2	53.0	9.8
11	131.3	111.0	-20.3	53.6	36.0	-17.6	508.8	508.0	-0.8	1081.2	1223.0	141.8
12	73.6	75.0	1.4	43.9	48.0	4.1	104.9	117.0	12.1	361.6	383.0	21.4
13	56.5	76.0	19.5	11.8	19.0	7.2	82.9	115.0	32.1	97.0	128.0	31.0
14	1.2	4.0	2.8	15.8	17.0	1.2	8.1	10.0	1.9	33.4	35.0	1.6
15	8.4	12.0	3.6	18.9	37.0	18.1	23.8	40.0	16.2	35.3	64.0	28.7
	Ave change:		9.79%	Ave change:		13.47%	Ave change:		13.37%	Ave change:		9.39%

The D_{max} values collected were obtained using the Eclipse and Elements software built-in measurement. All of the structures were designated as OARs in the Elements planning system and the brainstem was designated as the highest priority OARs. As such, the values shown for the Elements plans reflect the optimization algorithms consideration. Similarly, in the Eclipse plans, these OARs were also given manual consideration with respect to the dose delivered. However, because the plans were originally created in Eclipse, the arc lengths, couch positions,

and collimator angles were chosen with respect to the PTV, GTV and the OARs. Those same geometries being used in the Elements environment implicitly give the Elements plans the same considerations for the local structures and OARs that the Eclipse plans received.

Table 7: Gamma analysis of each QA for each treatment plan delivered to the MapCHECK stereoPHAN setup. The percentage passing rate of each pair of plans from the respective treatment planning systems are arranged into six separate combinations of percent difference at a point and distance to agreement combinations between the plans.

	3%/2mm		2%/2mm		1%/2mm		3%/1mm		2%/1mm		1%/1mm	
	Ecl.	Ele.	Ecl.	Ele.	Ecl.	Ele.	Ecl.	Ele.	Ecl.	Ele.	Ecl.	Ele.
1	0.992	1.000	0.980	1.000	0.976	1.000	0.988	1.000	0.951	0.992	0.951	0.973
2	1.000	1.000	1.000	1.000	1.000	1.000	1.000	1.000	0.989	1.000	0.989	0.990
3	1.000	1.000	1.000	1.000	0.995	1.000	1.000	1.000	0.995	1.000	0.988	0.991
4	1.000	1.000	1.000	1.000	1.000	1.000	1.000	1.000	1.000	1.000	1.000	1.000
5	1.000	1.000	0.995	1.000	0.995	0.995	0.986	1.000	0.971	0.995	0.967	0.980
6	1.000	1.000	1.000	1.000	1.000	1.000	1.000	1.000	0.989	1.000	0.989	0.990
7	1.000	1.000	1.000	1.000	1.000	1.000	1.000	1.000	1.000	1.000	1.000	1.000
8	1.000	1.000	1.000	1.000	1.000	1.000	1.000	1.000	1.000	1.000	1.000	1.000
9	1.000	1.000	1.000	1.000	1.000	1.000	1.000	1.000	0.985	1.000	0.985	1.000
10	1.000	1.000	1.000	1.000	1.000	1.000	1.000	1.000	1.000	1.000	0.990	1.000
11	0.992	0.995	0.992	0.994	0.990	0.990	0.992	0.995	0.990	0.992	0.985	0.988
12	0.994	0.995	0.990	0.993	0.984	0.986	0.994	0.995	0.984	0.986	0.980	0.980
13	0.993	0.997	0.977	0.988	0.960	0.982	0.987	0.997	0.964	0.982	0.930	0.966
14	1.000	1.000	1.000	1.000	0.994	1.000	1.000	1.000	1.000	1.000	0.990	0.991
15	0.983	1.000	0.970	1.000	0.970	0.995	0.974	1.000	0.953	0.989	0.944	0.963

Each plan received a patient specific QA plan delivery to analyze the amount of congruence between the calculated plan and actual treatment delivered. The results were given as a fraction of passing points in the calculated plan that were within one, two, and three percent of

the dose difference points of the delivered plan and within a 1mm or 2mm distance to agreement of another point in the delivered plan.

Table 8: Cubic volume of brain tissue receiving 12 Gy subtracting the PTV for each plan in each treatment planning system. % change represents the percentage of change from the Eclipse planning system to the Elements planning system in volume of brain tissue omitting the PTV.

	Eclipse V12 (cm^3) PTV subtracted	Elements V12 (cm^3) PTV subtracted	PTV (cm^3)	% change	cc change
1	1.22463	1.28	2.09	4.52%	0.06
2	0.7654	0.822	0.45	7.39%	0.06
3	0.601381	0.479	0.29	-20.35%	-0.12
4	1.21642	1.068	0.66	-12.20%	-0.15
5	0.7827	0.69	0.37	-11.84%	-0.09
6	1.23467	1.089	1.28	-11.80%	-0.15
7	0.74416	0.641	0.27	-13.86%	-0.10
8	0.87539	0.852	0.39	-2.67%	-0.02
9	0.624531	0.569	0.2	-8.89%	-0.06
10	0.503458	0.488	0.13	-3.07%	-0.02
11	4.7197	3.439	9.79	-27.14%	-1.28
12	3.65749	3.033	3.92	-17.07%	-0.62
13	2.77201	2.192	4.53	-20.92%	-0.58
14	1.10421	1.01	0.59	-8.53%	-0.09
15	1.93686	1.676	1.88	-13.47%	-0.26

The cubic volumes of tissue receiving at least 12 Gy in each pair of plans were compared. V_{12} has the tendency to correlate with radiation induced tissue necrosis and is considered a common metric for levels of tissue toxicity. However, some portion of V_{12} is the treatment volume itself so to more clearly show the amount of normal tissue irradiated by twelve Gray or more, the volumetric and percentage change were evaluated both including the PTV in V_{12} and subtracting it out.

Plots were also created to visualize scale of differences in V_{12} volume with respect to the PTV volume as well as the percentage change from Eclipse to Elements for the volume of normal brain tissue receiving at least twelve Gy.

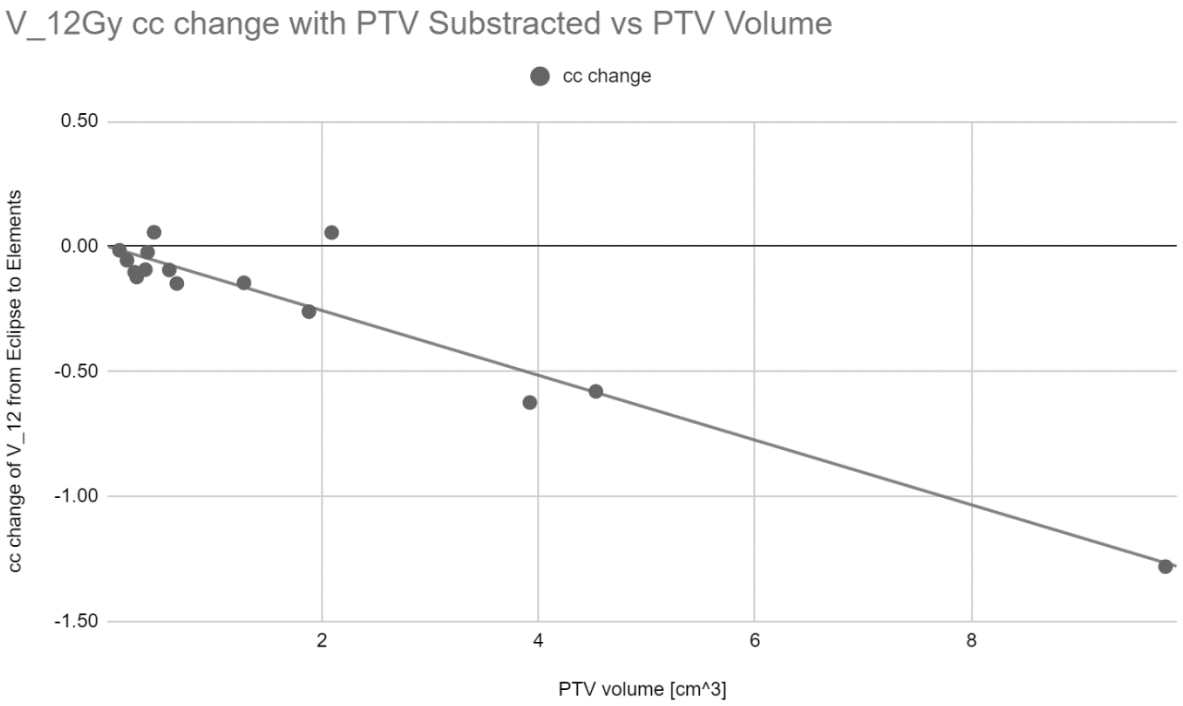

Figure 3: Plot detailing the scaling of the volume of tissue receiving at least 12 Gy with respect to the volume of the PTV. V_{12Gy} of the plans created in Elements are on average 5.7% lower in volume than the plans created in Eclipse.

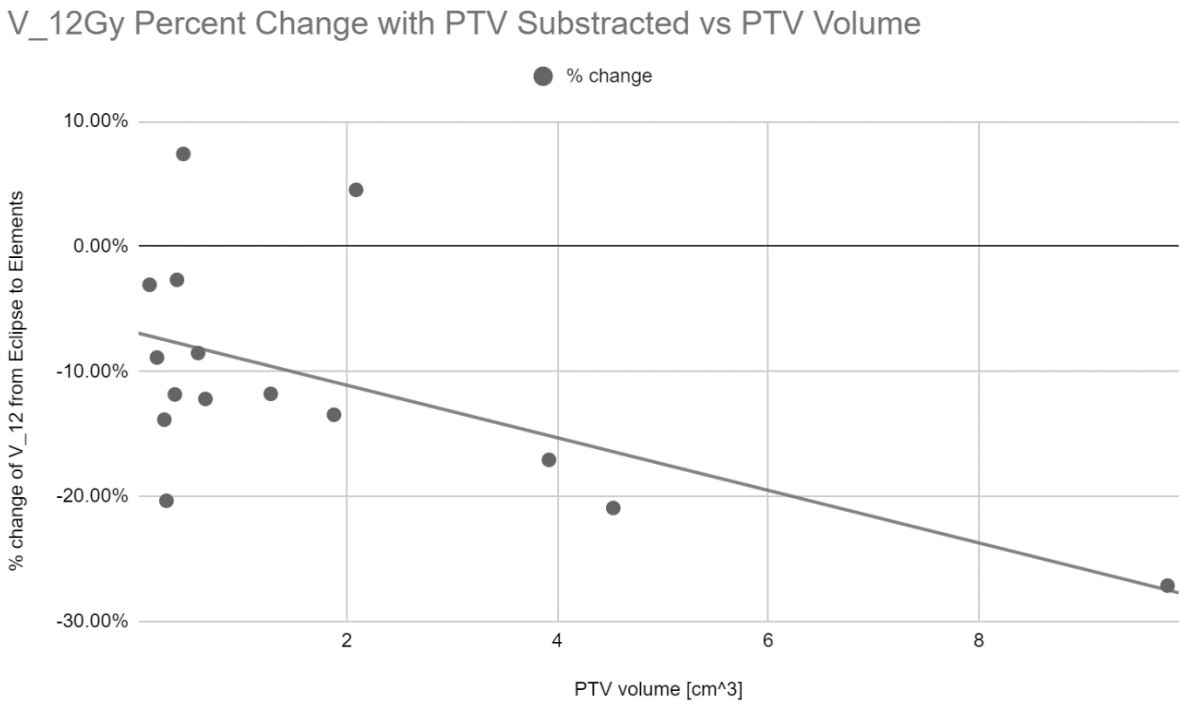

Figure 4: Plot of the percentage change in V_{12} from Eclipse to Elements with respect to PTV volume.

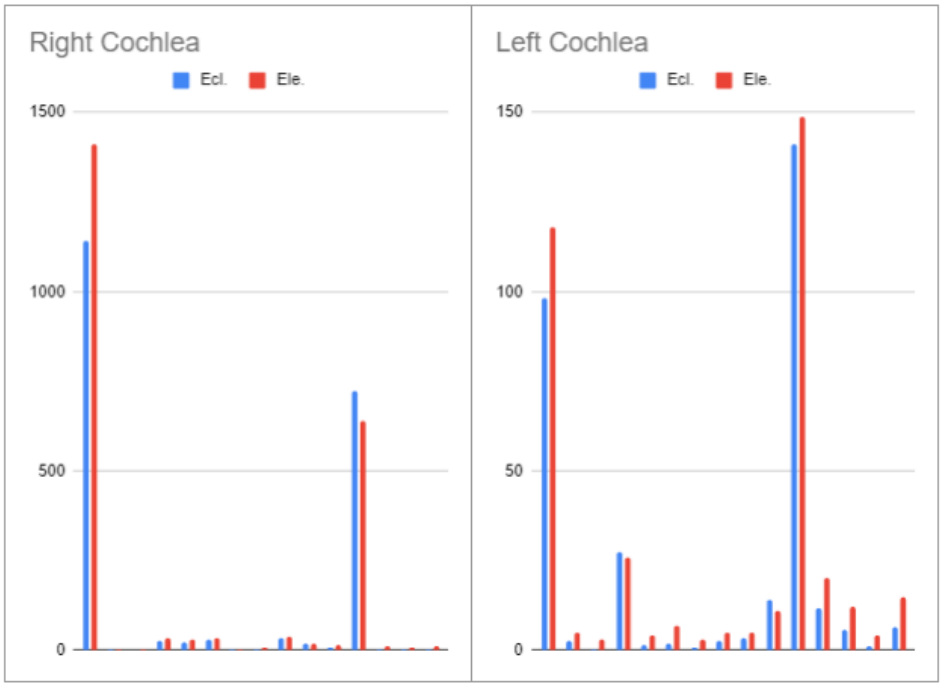

Figure 5: Comparison of each treatment plan delivery of D_{max} to OARs right and left cochlea.

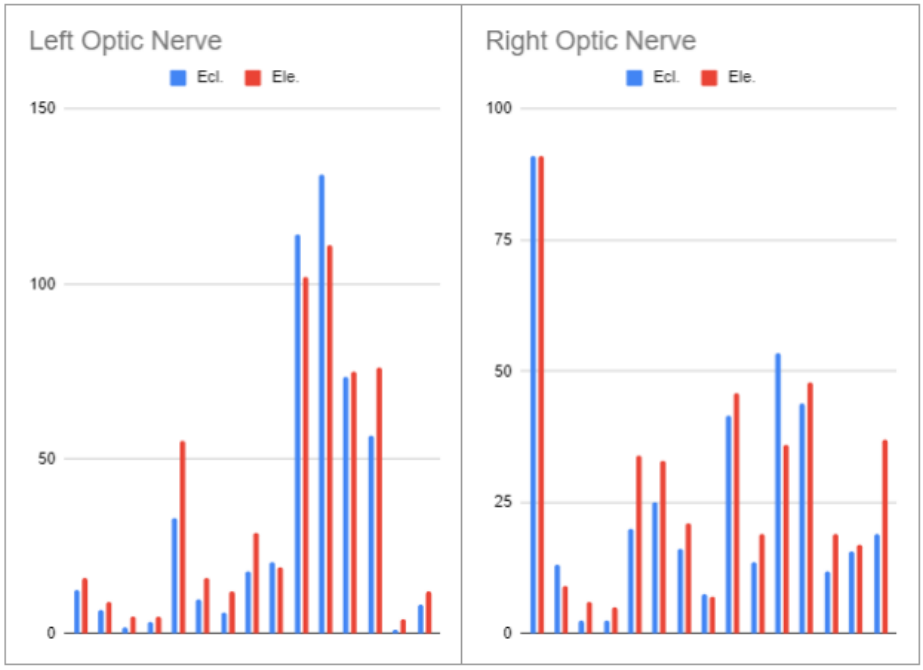

Figure 6: Comparison of each treatment plan delivery of D_{max} [cGy] to OARs left and right optic nerve.

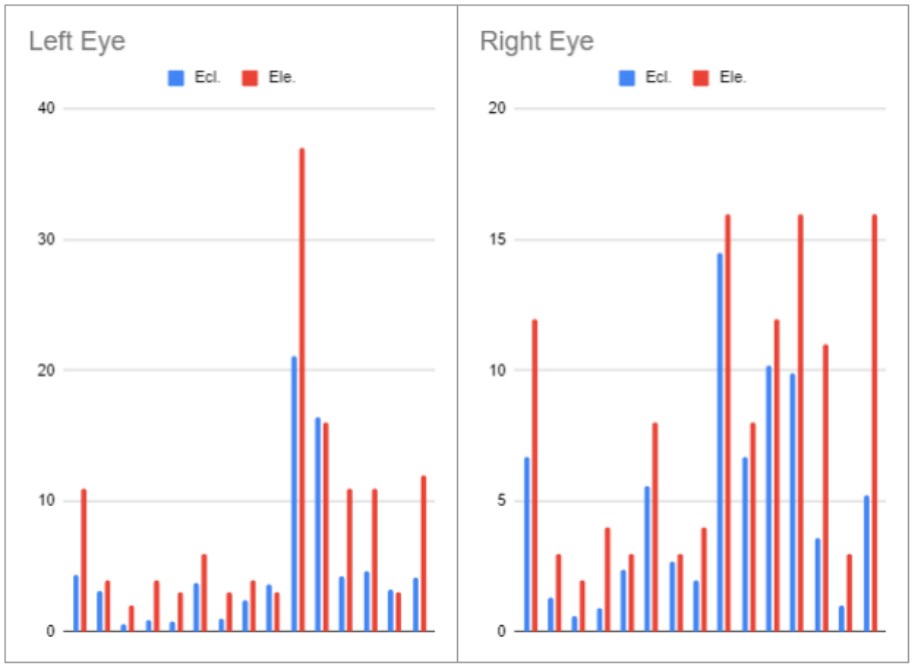

Figure 7: Comparison of each treatment plan delivery of D_{max} [cGy] to OARs left and right eyes.

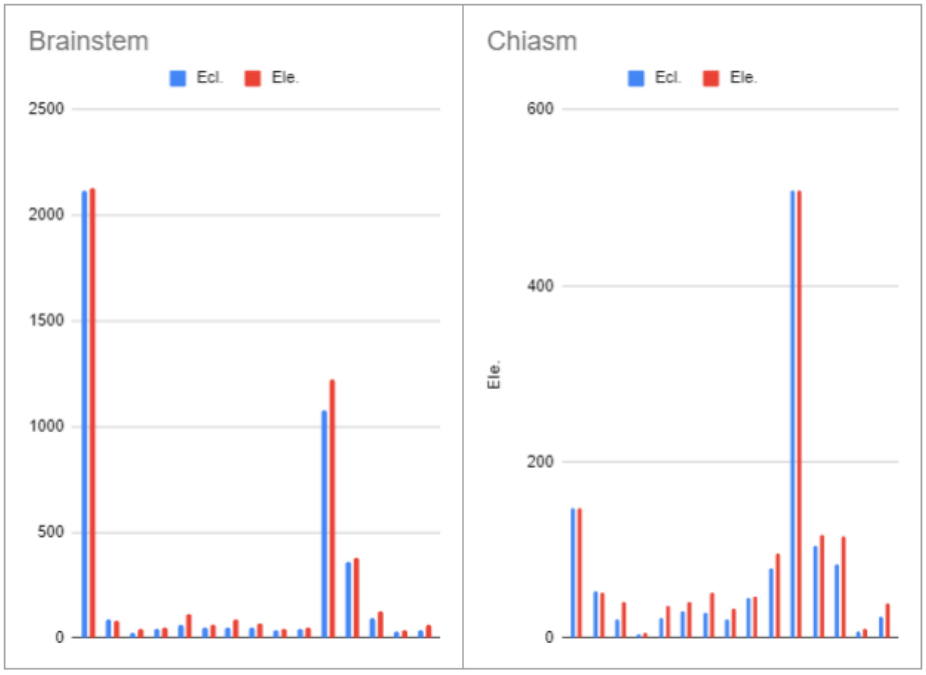

Figure 8: Comparison of each treatment plan delivery of D_{max} [cGy] to OARs left and right eyes.

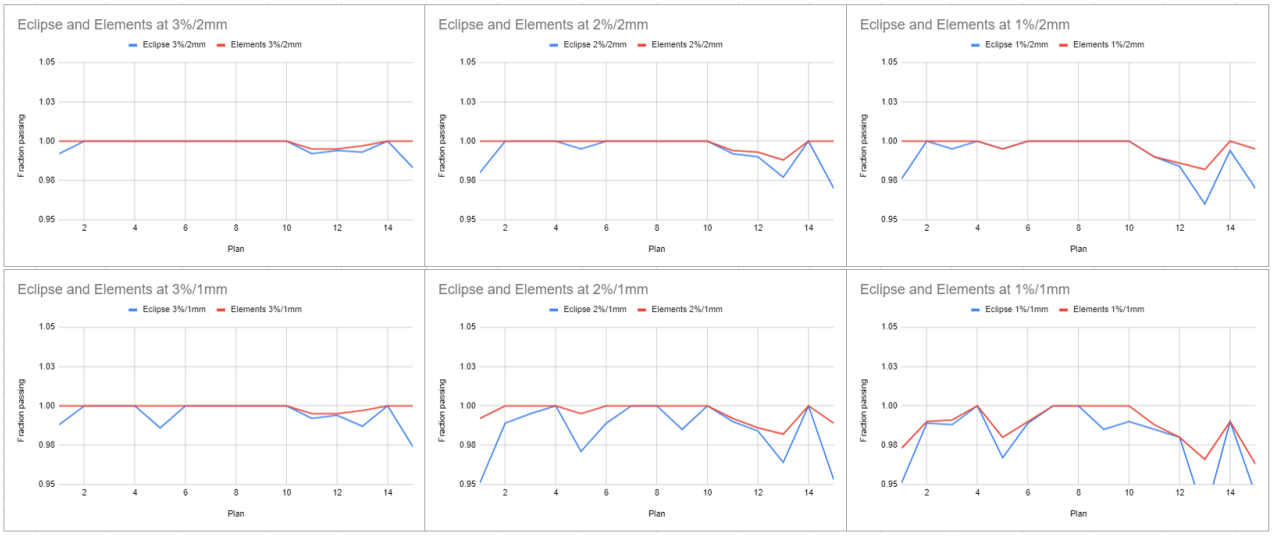

Figure 9: Gamma analysis for each of the combinations of percent dose difference at 1, 2, and 3% and distance to agreement at 1 mm and 2 mm.

4. Discussion

Table 4. is a summary of the measurements of the comparison parameters. The mean, median, standard deviation, and interquartile range were calculated for each set of measurements for each respective TPS and the statistical significance was for the median difference. Criteria with Wilcoxon test statistic values of 25 or less were labeled in bold to denote significant statistical difference between the Eclipse and Elements sets of data. All criteria aside from the total MUs delivered, the IPCI, and the D_{max} values for the right optic nerve were found to be significantly statistically different.

The inverse Paddick conformity index was used. Indices for each set of plans have very similar values with no statistical difference. An IPCI with a value of 1 is most desirable because it would indicate that the overtreatment and undertreatment ratios were both approaching a value of one. In this situation, the volume of treated tissue would be approaching the volume of the target tissue. Numerically, this is ideal as the target volume is the volume that should be treated.

However, an ideal value would be less than 1.18 [11]. Both the mean and median values of the Eclipse were just outside of this range at 1.19. The Elements plan IPCI values were just inside the ideal range with a mean of 1.16 and median of 1.12. Both sets of plans had quite small interquartile ranges at 0.04 and 0.06 showing a close distribution of index values. Given that there is no statistical difference between the two sets of plans, this indicates that each TPS is generating plans at about the ideal conformal limit for IPCI.

The gradient indices for each plan did show statistical difference from each other, though the scale was still small. Here, the standard deviation and interquartile range were smaller for the Elements plans showing more consistency in dose fall off. As a ratio of the 50% isodose line and the 100% isodose line, the gradient index is an indicator of how quickly dose is reduced in the

surrounding tissue moving away from the treatment area. The smaller indices for the Elements plans show that the dose, from a volumetric standpoint, does fall off more quickly. Though the gradient index value does not address how concentric or symmetrical the PTV and the 100% isodose volume are to each other, using the values in conjunction with the IPCI give a useful sense of how conformal a plan is.

Treating the IPCI values as effectively the same between the planning systems with no significant statistical difference, W = 34, and noting the small increase in performance of the Elements system gradient indices, it can be said the Elements TPS delivered more conformal treatment plans than the Eclipse system.

In Table 1. comparing the volumes of tissue receiving 12 Gy or more, it was shown that the mean value of V_{12Gy} was 6% lower at 3.31 cm^3 for the Elements plans and had a median value 7.1% lower at 1.57 cm^3 than the Eclipse plans. These values were shown to have significant statistical differences with a Wilcoxon test statistic of 12. V_{12Gy} scales semi-linearly with the PTV size, as can be seen in Figure 3. In general, the Elements plans have a 5.7% lower V_{12Gy} value than the plans created in Eclipse.

This difference is significant as V_{12Gy} is an important factor in predicting potential tissue necrosis in the brain [12]. These late effects are typically associated with neurological complications and reducing the total tissue exposed to 12 Gy is a chance to reduce the risk of those complications. With exception of two cases, the Elements planning system consistently outperformed Eclipse in every other case.

The difference in total MUs delivered for each set of plans was found statistically insignificant with a Wilcoxon test statistic of 40. This test was chosen due to the non-normal distribution of the data established with the Shapiro-Wilks test. In general, Elements delivered

slightly less MUs than eclipse with 2.4% less on average and a 6.3% small median. The interquartile range of the Elements plans was also 17.3% smaller than Eclipse plans.

Looking at the D_{max} values for the organs at risk in Table 1. the differences between the plan sets were all found to be statistically significant with the exception of the right optic nerve, having a Wilcoxon test statistic of 28>25. The Eclipse plans were 10.1% lower in average dose delivered to the other OARs. This could possibly be the result of forcing the matched geometries selected by the dosimetrist in the Elements environment. Utilizing the arc trajectory optimization that was avoided in this study would allow for Elements to potentially choose more effective treatment delivery geometries that better suited the other optimization processes.

Context is important when evaluating these criteria. For instance, in Table 6. It can be seen that in case 3 there is a 328.57% increase in the D_{max} value for the Elements plan but this percentage increase is only from 0.7 cGy to 3 cGy. Similar instances of this can be found when looking at the right and left eyes, showing large increases in percentage but actually quite small increases in dose. When looking at the left and right optic nerves, the mean D_{max} for both Eclipse and Elements is far below a single Gy. While there is some debate concerning what dose level might be appropriate to avoid optic neuropathy, below one Gy is well within suggested tolerances at 8-10 Gy. Figures 5, 6, 7, and 8 show the dose in cGy to OAR for each paired case, sorted by structure. It is easy to see that despite large percentage increases to some of the doses to OARs, most instances of increase are inconsequential. Increased reliance on the Elements optimizations could further reduce the dose to OARs.

One place the Elements system was challenged in this study was case 1 with the dose to the right cochlea. Shown in Figure 5, it can be seen there is a substantial increase of dose deposition to the cochlea compared to the Eclipse plan. In this case, the lesion was laterally

against the brainstem, so increased irradiation of the brainstem was unavoidable, as shown in Table 6 and Figure 8. Here, the brainstem was given the designation of most important OAR in the Elements TPS when calculating the dose. This was done to minimize the unavoidable increase in dose to the brainstem due to the location of the lesion. Elements perform quite well, showing only a 0.61% increase in dose. However, the OAR priority of the right cochlea was not weighted as heavily and consequently was not considered with enough importance in the optimization. The consequence was a 23.59% increase of almost 270 cGy to the cochlea. Increasing the Guardian setting and reducing the D_{max} value in Elements could put more pressure on the algorithm to spare the structure more efficiently

Considering the instance in case 12 of the right cochlea, a different result can be seen. Elements provided an 11.62% reduction in dose delivered to the OAR, dropping from 723 cGy to 639 cGy. Here, the optimization was more appropriately considering the OAR and able to reduce the dose. The fixed arc lengths and couch positions copied over from Eclipse plans also had a less negative intrinsic impact on the OAR dose.

In general, out of the 8 OARs across 15 treatments for a total 120 OAR considerations for each TPS, only one instance of the brainstem and one instance of the cochlea superseded conventional dose constraint values. These superseding doses were present in both Eclipse and Elements, meaning that even with manual consideration, the dose constraints could not be met. In this respect, Elements has delivered comparable OAR sparing to the Eclipse plans and with more time spent optimizing the plan, this could be further improved.

Gamma analysis was performed on each calculated plan and the respective measured plan. The analysis was carried for 1%, 2%, and 3% dose differences and 1- and 2-mm distance to agreement criteria. While the Eclipse plans delivered an acceptable level of coincidence between

the calculation and the delivered beam, verification of the Elements plans was consistently higher. Every Elements plan outperformed its counterpart Eclipse plan with gamma analysis, always resulting in a higher pass rate each time. Shown in Table 7 it can be seen that these higher pass rates were regularly 100%. As spatial tolerance decreased, cases with larger PTV showed instances of increased failure points. This visible trend in Figure 9 was also present and quite visible for decreasing percent dose difference tolerance at both the 1 mm and 2 mm distance to agreement.

4.1 Future work

A great deal of future work can be done moving forward. Further exploration of the optimization algorithms may effectively address instances where Elements falls short in comparison to Eclipse. In the interest of being able to compare the two sets of plans directly in this study, the geometries were matched in the Elements environment, using the arc rotations and couch positions exactly as they were in the Eclipse system. In order to achieve this, the trajectory optimization was intentionally not utilized in order to preserve the copied geometries. A logical next step would be to allow the algorithm to become active and influence the gantry rotation and couch position values. This addition to the set of optimizations may increase the effectiveness of the other optimizations by simply considering them from new treatment delivery positions.

Here, it would also be ideal to increase the population size to increase the data set and perhaps even explore the impact of PTV size and location on the algorithms' effectiveness. That effectiveness could also be explored using protocols with fewer arcs. If the TPS could create a deliverable plan with fewer arcs, this would be advantageous to the patient who would then need

to be treated for less time as well as the department by reducing the overall treatment time and potentially increasing patient throughput.

Finally, a true test of efficiency of the Elements TPS would be to include the process of contouring structures. This study relied on the structure sets created in Eclipse and required the import of those structures into the Elements planning software before any planning could occur. Including the contouring process of the Elements TPS would potentially reduce the time moving from one TPS to another. Using the auto-contouring feature in Elements may also further reduce the overall total time spent contouring.

5. Summary and Conclusions

The work done here investigating the efficacy of the BrainLab Elements TPS and how it dosimetrically compares in the treatment planning process to the Eclipse planning system has demonstrated that Elements is a competitive alternative to the Eclipse TPS. The Elements TPS was found to have similar conformality and improved gradient indices. The volume V_{12Gy} was reduced in 13 of the 15 the cases showing favorable improvement over Eclipse and potential for reduced radiation induced tissue necrosis.

D_{max} to OARs was increased for the Elements plans but in general, these increases were well below acceptable dose constraints. Instances where they were not below the constraint were also instances where the Eclipse plan also failed. It is possible that the increased dose could be controlled by raising priorities and settings of the algorithms and should be explored in the future.

Gamma analysis demonstrated superior coincidence between the Elements calculations and the delivered treatments, beating out Eclipse in every treatment, across every percent dose difference and every distance to agreement. These results suggest that the Elements calculations and expected treatment delivery are well within the mechanical constraints of the linear accelerator delivering the plan. The workflow and streamlined planning approach coupled with the promising performance of the plans explored will offer a viable alternative to Eclipse for cranial SRS treatment planning.

6. Citations

[1] Churilla, Thomas M., et al. "Comparison of local control of brain metastases with stereotactic radiosurgery vs surgical resection: a secondary analysis of a randomized clinical trial." *JAMA oncology* 5.2 (2019): 243-247.

[2] Colaco, Rovel J., et al. "A contemporary dose selection algorithm for stereotactic radiosurgery in the treatment of brain metastases—An initial report." *Journal of Radiosurgery and SBRT* 4.1 (2016): 43.

[3] McDermott, Patrick N., and Colin G. Orton. *The physics & technology of radiation therapy*. Madison: Medical Physics Publishing, 2010.

[4] Tallet, Agnes V., et al. "Neurocognitive function impairment after whole brain radiotherapy for brain metastases: actual assessment." *Radiation Oncology* 7.1 (2012): 1-8.

[5] Failla, Gregory A., et al. "Acuros XB advanced dose calculation for the Eclipse treatment planning system." *Palo Alto, CA: Varian Medical Systems* 20 (2010).

[6] Knill, Cory, et al. "Commissioning cranial single-isocenter multi-target radiosurgery for the Versa HD." *Journal of Applied Clinical Medical Physics* 22.4 (2021): 108-114.

[7] Paddick, Ian. "A simple scoring ratio to index the conformity of radiosurgical treatment plans." *Journal of neurosurgery* 93.supplement_3 (2000): 219-222.

[8] Paddick, Ian, and Bodo Lippitz. "A simple dose gradient measurement tool to complement the conformity index." *Journal of neurosurgery* 105.Supplement (2006): 194-201.

[9] Hanusz, Zofia, Joanna Tarasinska, and Wojciech Zielinski. "Shapiro-Wilk test with known mean." *REVSTAT-Statistical Journal* 14.1 (2016): 89-100.

[10] Ohtakara, Kazuhiro, S. Hayashi, and H. Hoshi. "The relation between various conformity indices and the influence of the target coverage difference in prescription isodose surface on these values in intracranial stereotactic radiosurgery." *The British journal of radiology* 85.1014 (2012): e223-e228.

[11] Torrens, Michael, et al. "Standardization of terminology in stereotactic radiosurgery: Report from the Standardization Committee of the International Leksell Gamma Knife Society: special topic." *Journal of neurosurgery* 121.Suppl_2 (2014): 2-15.

[12] Minniti, Giuseppe, et al. "Stereotactic radiosurgery for brain metastases: analysis of outcome and risk of brain radionecrosis." *Radiation oncology* 6.1 (2011): 1-9.

[13] Torrens, Michael, et al. "Standardization of terminology in stereotactic radiosurgery: Report from the Standardization Committee of the International Leksell Gamma Knife Society: special topic." *Journal of neurosurgery* 121.Suppl_2 (2014): 2-15.

[14] Velten, Christian, et al. "Single isocenter treatment planning techniques for stereotactic radiosurgery of multiple cranial metastases." *Physics and imaging in radiation oncology* 17 (2021): 47-52.

[15] Minniti, Giuseppe, et al. "Stereotactic radiosurgery for brain metastases: analysis of outcome and risk of brain radionecrosis." *Radiation oncology* 6.1 (2011): 1-9.

[16] Menon, Sharika Venugopal, et al. "Evaluation of plan quality metrics in stereotactic radiosurgery/radiotherapy in the treatment plans of arteriovenous malformations." *Journal of medical physics* 43.4 (2018): 214.

[17] Vergalasova, Irina, et al. "Multi-institutional dosimetric evaluation of modern day stereotactic radiosurgery (SRS) treatment options for multiple brain metastases." *Frontiers in oncology* 9 (2019): 483.

[18] Hellerbach, Alexandra, et al. "Radiotoxicity in robotic radiosurgery: proposing a new quality index for optimizing the treatment planning of brain metastases." *Radiation Oncology* 12.1 (2017): 1-9.

[19] Brodin, N. Patrik, and Wolfgang A. Tomé. "Revisiting the dose constraints for head and neck OARs in the current era of IMRT." *Oral oncology* 86 (2018): 8-18.

[20] Mayo, Charles, et al. "Radiation dose–volume effects of optic nerves and chiasm." *International Journal of Radiation Oncology* Biology* Physics* 76.3 (2010): S28-S35.